

Article

Influence of Micro- and Macrostructure of Atomised Water Jets on Ammonia Absorption Efficiency

Wiktor Waśnik ¹, Małgorzata Majder-Łopatka ²  and Wioletta Rogula-Kozłowska ^{2,*} 

¹ Faculty of Safety Engineering and Civil Protection, The Main School of Fire Service, 52/54 Slowackiego Street, 01-629 Warsaw, Poland

² Institute of Safety Engineering, The Main School of Fire Service, 52/54 Slowackiego Street, 01-629 Warsaw, Poland

* Correspondence: wrogula@sgsp.edu.pl

Abstract: Ammonia has a very wide range of applications. Its worldwide production exceeds 230 million tonnes per year. Due to its properties, ammonia causes a serious threat to human life and health when released uncontrolled into the environment. Research carried out in the work shows that this substance may be effectively neutralised by absorption in water. The aim of research described in this paper is to determine the influence of key parameters of the micro- and macrostructure of water streams on the course of the ammonia absorption process. During the studies, different types of water nozzles were used, with similar efficiency and supply pressure, but characterised by different parameters of the micro- and macrostructure of the produced stream. The experiments were divided into two stages. In the first one, the macro- and microparameters of the streams were measured, while in the second one, the changes in ammonia concentration were established during delivering spray jet generation by different nozzles. Among the basic parameters of the macrostructure, the spray angle and liquid distribution in the jet (spray intensity) were determined, while for the microstructure, the droplet size distribution and mean droplet diameters were measured. Ammonia concentration was measured by means of a photoionisation detector (PID). In order to evaluate the absorption efficiency of different water spray jets, the apparent absorption rate (k_p) and the half-time of concentration reduction ($t_{1/2}$) in the kinetic range were established. The study has confirmed that atomised water jets are an effective method for neutralising ammonia released into the environment. The research has a practical aspect and shows that the structure of atomised water streams influence the course of the absorption process. Increasing the spray angle in a conical stream leads to an improvement in the quality of water atomisation and helps increase ammonia absorption. Moreover, it was also observed that for the absorption of spatial ammonia clouds, use should be made of nozzles generating streams with full spray cones and high uniformity of spray and dispersion.



Citation: Waśnik, W.; Majder-Łopatka, M.; Rogula-Kozłowska, W. Influence of Micro- and Macrostructure of Atomised Water Jets on Ammonia Absorption Efficiency. *Sustainability* **2022**, *14*, 9693. <https://doi.org/10.3390/su14159693>

Academic Editor: Elena Cristina Rada

Received: 21 June 2022

Accepted: 1 August 2022

Published: 6 August 2022

Publisher's Note: MDPI stays neutral with regard to jurisdictional claims in published maps and institutional affiliations.



Copyright: © 2022 by the authors. Licensee MDPI, Basel, Switzerland. This article is an open access article distributed under the terms and conditions of the Creative Commons Attribution (CC BY) license (<https://creativecommons.org/licenses/by/4.0/>).

Keywords: absorption; ammonia; water spray; spray intensity; droplet size distribution; spray jets; ammonia contamination; release of ammonia into the environment

1. Introduction

Given its toxic and corrosive properties, in the event of uncontrolled release, ammonia (NH₃) poses a serious hazard for people and for the environment [1,2]. Contact with ammonia may cause burns to the skin, eyes and respiratory mucous membranes, while prolonged exposure may cause pulmonary oedema and even death [3]. Ammonia has a very wide range of applications. Among other things, it is used to produce artificial fertilisers, synthetic fibres, cosmetics, nitric acid [4] and medications [5]; it is also used in industrial refrigeration [6]. In Poland, ammonia production is quite substantial and in the last decade amounted to approximately 1.5% of global production and approximately 15% of production in countries of the European Union [7,8]. A summary of annual ammonia production in Poland for the period 2015–2020 is presented in Figure 1.

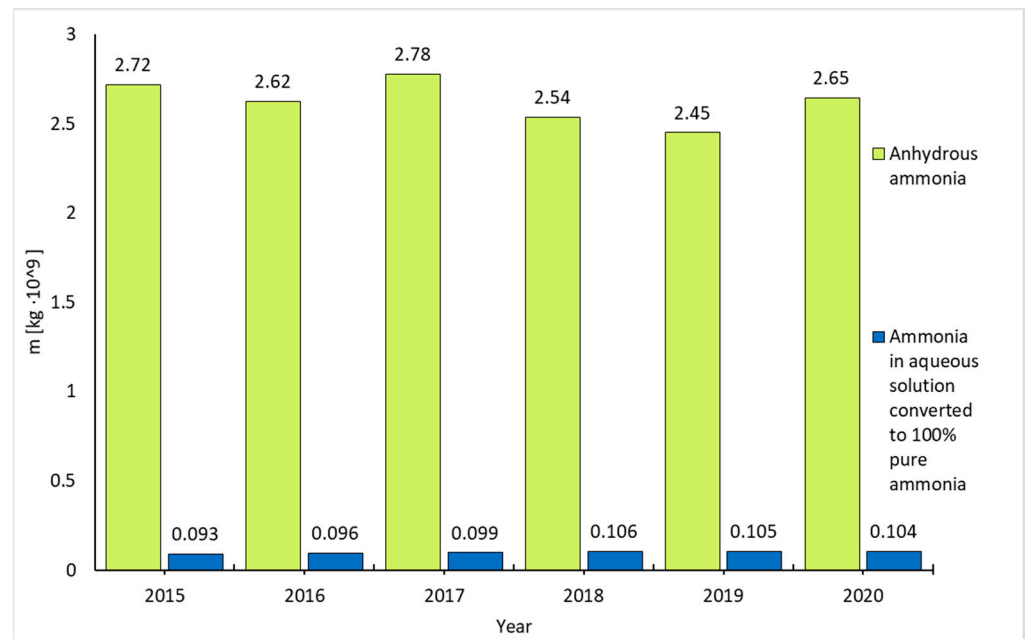


Figure 1. Production of ammonia in Poland in the period 2015–2020. Source: own study based on [7].

It should be emphasised that NH_3 is also uncontrollably produced and emitted into the environment in the automotive industry and in animal husbandry [9].

Furthermore, ammonia emissions give rise to intensified air pollution by particulate matter because, as a primary airborne neutraliser, it is part of the fine particulate matter (mainly $\text{PM}_{2.5}$) of secondary inorganic aerosol in the atmosphere, and is furthermore responsible for much of the deposition of nitrogen compounds in ecosystems [10].

Numerous studies conducted both in Poland [11–17] and abroad [18–23] prove that water sprays are an inexpensive and effective method of limiting the effects of accidents in which hazardous gases are involved by reducing their concentration. The process of absorbing a gaseous substance throughout the volume of a liquid substance is called absorption and is the primary means of neutralising gaseous pollutants. The fundamental steps of absorption are: transfer of the component to the liquid surface, dissolution in the boundary layer at the liquid surface and transfer of the absorbed component into the liquid [24–26]. The absorption efficiency of hazardous substances in water is strictly related to their water solubility, reactivity and rate of diffusion into the droplet [15,22]. Studies show that ammonia, as a highly water-soluble substance, is absorbed in a highly efficient way by water streams [14,17]. The drop of NH_3 concentration during the dispersed stream feeding is almost of an exponential character, which points to the fact that the rate of the absorption process is directly proportional to ammonia concentration. The course of the process from the kinetic viewpoint can be described according to the pseudo-first order kinetic reaction and expressed by the following differential equation [16]:

$$-\frac{d[C]}{d[t]} = k_p[C] \quad (1)$$

where:

C —concentration of ammonia in the chamber [ppm],

k_p —apparent constant for the absorption process rate [s^{-1}].

t —time [s].

Apart from the apparent constant for the absorption process rate, an important parameter characterising this process is the concentration half-time, denoted as $t_{1/2}$ and expressed by the following formula [15]:

$$t_{1/2} = \frac{\ln 2}{k_p} \quad (2)$$

where:

$t_{1/2}$ —the concentration half-time [s].

k_p —apparent constant for the absorption process rate [s^{-1}].

In ammonia absorption, the value of k_p and $t_{1/2}$ is influenced by many factors related to the water feed and its parameters. Among these, the following are particularly important: water temperature [17], initial ammonia concentration, the type of spray nozzle and its supply pressure [12].

The aim of studies presented in this paper is to determine the influence of key micro- and macrostructure parameters of atomised streams on the process of ammonia absorption in water. Water nozzles of various types were used in the study. The nozzles had similar capacity and supply pressure, but were characterised by different parameters of the micro- and macrostructure of the produced stream. Among the basic parameters of the macrostructure, the following are mentioned in available literature sources: jet range, spray angle, flow coefficient and liquid distribution in the jet (spray intensity), while in the case of the microstructure, these are: droplet size distribution and mean droplet diameters [27,28].

2. Materials and Methods

The experiments were divided into two stages. In the first stage, macroparameters of the atomised streams (the spray angle and spray intensity) were evaluated, and the microparameters were measured. In the second stage, it was established how the concentration of ammonia in the test chamber changes during the administration of spray streams produced by different nozzles.

The tests were carried out on a dedicated installation that was designed and built to perform research, the diagram of which is shown in Figure 2.

The following were used to disperse water:

- spiral nozzle TF 6 FCN with full sprinkling cone and max. spray angle of 90° [29],
- spiral nozzle TF 6 NN with full sprinkling cone and max. spray angle of 60° [29],
- nozzle NF 15 with a flat spray jet and a spray angle of approx. 65° [30].

The study of the spray angle was carried out by taking photographs of the jet, against the background of a board with reference dimensions, using the photographic method. The photographic documentation was analysed in a graphics programme, and the uncertainty of measurement was $\pm 2^\circ$.

The spraying intensity was tested using the bucket method. Water was collected in cylindrical measuring containers with a diameter of 64.5 mm and weighed on a balance with a range of up to 2 kg and an accuracy of 0.01 g. Water was dispensed until at least one the container was filled to a specified level. The spray intensity test was carried out for one quarter of the nozzle spray area. The measuring points were arranged according to the diagram shown in Figure 3. In all tests, the distance of the nozzle outlet from the plane formed by the upper edges of the measuring containers was 1000 ± 50 mm.

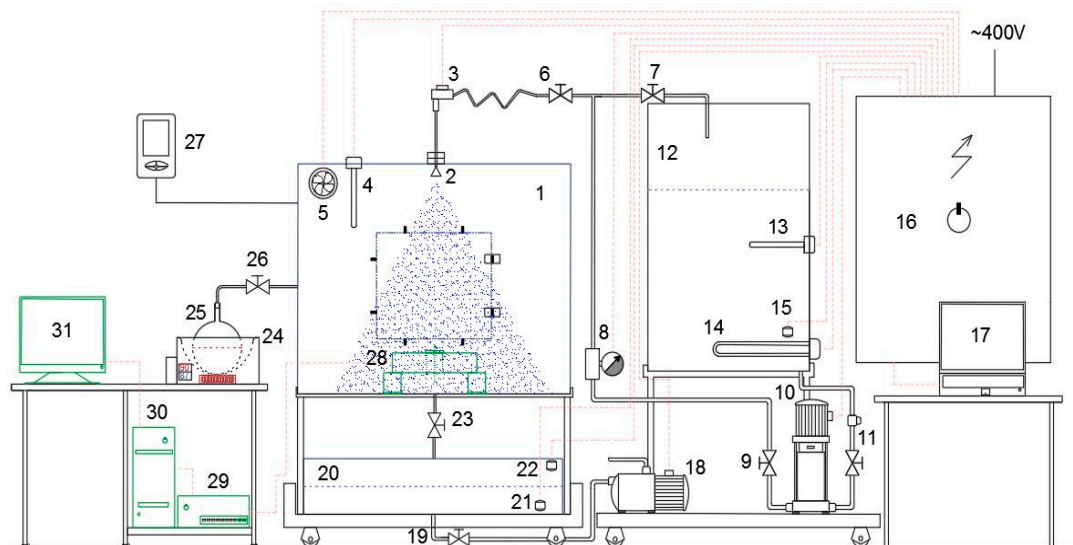


Figure 2. Test bench diagram: 1—transparent polymethyl methacrylate test chamber in the shape of a cube with a side length of 1.2 m, 2—spray nozzle, 3—pressure sensor WIKA S-20, 4—temperature sensor, 5—mixer, 6—main nozzle supply valve, 7—circulating line valve, 8—electromagnetic flow meter, 9—feed pump main valve, 10—feed pump main valve, 11—feed pump suction line, 12—water tank, 13—water temperature sensor, 14—heater, 15—water level sensor in tank, 16—signal and power supply cabinet, 17—main computer of the workstation with special software, 18—discharge pump with outlet to the sewerage system, 19—drainage valve of the water discharge tank, 20—water discharge tank, 21—sensor of low water level in the tank, 22—sensor of high water level in the tank, 23—test chamber drainage valve, 24—heating bowl, 25—round bottom flask with ammonium hydroxide (25% solution), 26—ammonia vapour shut-off valve, 27—multi-gas meter, 28—droplet diameter analyser probe, 29—printer, 30—computer, 31—screen. Source: own study.

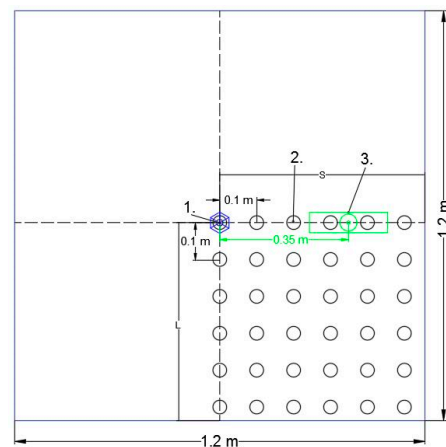


Figure 3. Arrangement of measuring points during testing of sprinkling intensity and microstructure parameters (top view of the test chamber base). Description of the drawing: 1—position of the nozzles and the measuring probe for testing the microstructure parameters of the spray jet produced using the NF 15 nozzle, 2—measuring containers for testing the spray intensity, 3—position of the measuring probe for testing the microstructure parameters of the spray jets of spiral nozzles. Source: own study.

Based on the mass of water collected in the measuring container, the intensity of sprinkling was calculated at each point. The sprinkling intensity was determined by the formula [31]:

$$I_z = \frac{m}{\zeta \cdot t \cdot A} \quad (3)$$

where:

- I_z —spray intensity [mm/min],
- m —weight of water collected [g],
- ζ —density of water at a temperature of 20 °C [g/mm³],
- t —water feed time [min],
- A —inlet area of the measuring vessel.

Testing of the microstructure of atomized water jets was carried out with the use of the IPS Droplet Spectrum Analyzer (KAMIKA Instruments Sp. z o.o. Sp.k, Warsaw, Poland). The functioning of this instrument makes use of the photoelectric method [32]. The electronic circuit of the device placed inside the measuring probe converts the light signal into an electrical impulse corresponding to a given droplet diameter. The change in the light signal is induced by the passage of droplets through the measuring probe space [33]. The IPS Droplet Spectrum Analyzer is able to measure droplets with diameters ranging from 0.5 µm to 3000 µm, while the accuracy of the measurements depends on the number of collected droplets. Based on the manufacturer's declaration and literature data [32], an accuracy of ±2% was assumed in microstructure measurements. The data recording time was 3 min, which made it possible to count more than 80,000 droplets. The following microstructure parameters were determined in the study: the droplet size distribution in terms of surface diameter, mean quantitative diameter, mean surface diameter, mean volumetric diameter and maximum surface diameter. The maximum surface diameter $D_{S0.9}$ is an important parameter that provides information as to the homogeneity of the dispersion, determined from the distribution of the jet. The diameter of $D_{S0.9}$ is a value, for which 90% surface formed in the spectrum are droplets with diameters smaller than $D_{S0.9}$ [27,34].

The structure of the diffused jet depends on the type of nozzle and the quantity and pressure of the flowing liquid [35,36]. A change in pressure has little effect on the spray angle, but significantly changes the spray intensity parameter, the droplet size distribution in jet and the mean and maximum droplet diameters [31,37,38]. In order to eliminate the influence of the supply pressure, all tests were performed at the nozzle supply pressure of 0.3 ± 0.002 MPa. The water supply system used and the design of the nozzles made it possible to achieve similar average capacities (350 ± 18 dm³/h).

The efficiency of ammonia absorption was evaluated on the basis of measurements of NH₃ concentration in the test chamber (Figure 2) during the administration of spray streams with defined micro and macro structure parameters. In each test, the initial ammonia concentration was 1000 ppm ± 50 ppm and the water temperature equalled 20 ± 1 °C.

An MX6 iBrid multigas detector (Industrial Scientific, Pittsburgh, PA, USA) with an electrochemical ammonia sensor and a photoionization detector was used to measure the ammonia concentration [39]. The aim of applying two different measurement techniques was to limit the influence of disturbances described in the literature data [40–42].

3. Results and Discussion

The conducted testing allowed the establishing of nozzle spray angles: TF 6 NN-57°, TF 6 FCN-85° and NF 15-58° (Figure 4). Spiral nozzles produce a cone-shaped spray pattern, whereas the NF 15 produces a flat jet in the shape of an isosceles triangle. The spraying angle is a very important parameter affecting the distribution of spraying intensity in streams generated by water nozzles and determines the spray surface. It has been observed that the side edges of the spray cone of the spiral nozzles become considerably narrower as the vertical distance from the nozzle increases. This is particularly evident in a nozzle with a larger dispersion angle (TF6 FCN). The value of the spray angle affects the number of nozzles and their distribution in protected areas [43]. This determines the spacing of the nozzles and their distance from the surface to be sprayed [34]. However, the research carried out indicates that the actual shape and dimensions of the jet should be taken into account when designing sprinkler systems, and not merely the spraying angle. The

determined spray angles may not reflect the correct spray surfaces, especially at greater distances from the nozzle.

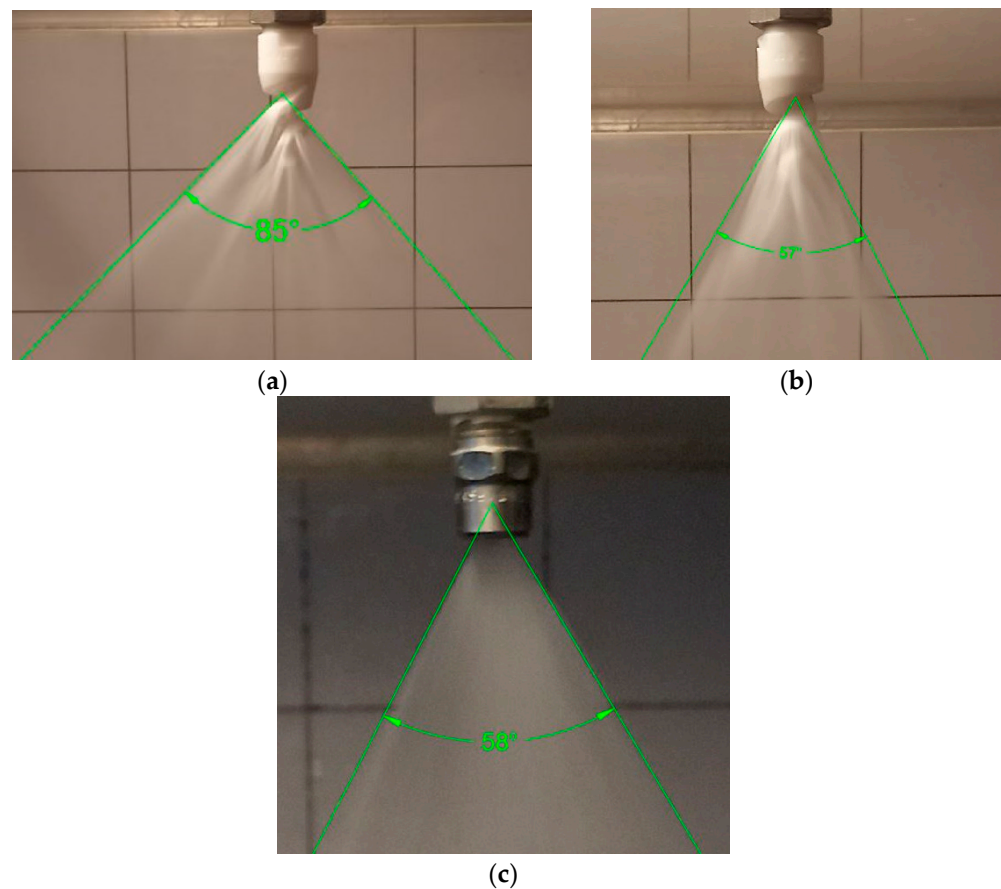


Figure 4. Established spray angle for nozzle: (a) TF 6 FCN, (b) TF 6 NN, (c) NF 15. Source: own study.

The resulting spray intensity values expressed in mm/min are shown in Table 1, while the intensity distributions are shown in Figure 5.

The NF 15 nozzle is characterised by a small spray area in the shape of a strip of small width. Nevertheless, the water intensity in the spray zone is very high, and for the highest values, obtained directly under the nozzle, it is more than 80 mm/min. However, the volume of the spray jet, and consequently the area of interaction between water and ammonia, is small.

Spiral nozzles have a sprinkling surface similar to a circle. The sprinkling surfaces obtained for both the TF 6 NN and TF 6 FCN nozzles are characterised by significantly lower spraying intensities in the zone directly under the nozzle than NF 15. Both spiral nozzles have a characteristic spray ring with the largest I_z values recorded at a distance of ca. 0.35 m from the SL (0.0) point located directly under the tested nozzle. The tested spiral nozzles have a similar sprinkling surface. A slightly larger area was ascertained for the TF 6 FCN nozzle having a larger spray angle. The small differences in the established sprinkling areas most likely arise from the sharp decrease in the velocity of droplet movement as they move away from the nozzle outlet. As can be seen from study [43], the geometry and flow parameters of the jet affect the velocity profile inside the spray only for small distances from the nozzle outlet. At greater distances from the nozzle, the velocity of liquid movement is so low that the jet turns into a gravitational descent. Executed studies of the spraying intensity of spiral nozzles indicate that an increase in the spray angle significantly affects the uniformity of sprinkling. This is confirmed by the maximum values obtained in the basic spray ring, which are more than twice as low for a nozzle with a higher spray angle (TF6 FCN).

Table 1. Nozzle intensity values at individual measuring points.

Nozzle Type		TF6 NN		average pressure		0.3 ± 0.002 MPa	
Application time		240 s		average capacity		350 ± 18 dm ³ /h	
Distance		S [m]					
		0.0	0.1	0.2	0.3	0.4	0.5
L [m]	0.0	2.127	1.870	3.616	7.819	5.823	1.524
	0.1	1.813	2.334	5.132	8.419	5.034	1.827
	0.2	2.735	3.234	4.673	9.106	3.418	1.237
	0.3	12.115	11.546	2.389	1.555	1.053	0.553
	0.4	20.980	15.914	4.017	1.078	0.383	0.228
	0.5	6.180	11.878	4.521	3.547	0.260	0.132
Nozzle type		NF15		average pressure		0.3 ± 0.002 MPa	
Application time		60 s		average capacity		350 ± 18 dm ³ /h	
Distance		S [m]					
		0	0.1	0.2	0.3	0.4	0.5
L [m]	0	83.369	71.438	54.955	33.662	30.403	12.121
	0.1	9.848	6.913	6.854	7.415	4.800	1.208
	0.2	0.464	0.539	0.493	0.562	0.392	0.278
	0.3	0.444	0.372	0.219	0.248	0.173	0.085
	0.4	0.291	0.291	0.183	0.170	0.131	0.046
	0.5	0.232	0.101	0.127	0.085	0.065	0.046
Nozzle type		TF6 FCN		average pressure		0.3 ± 0.002 MPa	
Application time		600 s		average capacity		350 ± 18 dm ³ /h	
Distance		S [m]					
		0	0.1	0.2	0.3	0.4	0.5
L [m]	0	1.687	2.627	3.356	3.069	1.770	0.598
	0.1	1.662	2.308	3.040	2.897	1.482	0.454
	0.2	2.487	3.837	3.883	3.240	1.647	0.482
	0.3	3.407	7.796	5.873	2.315	0.991	0.415
	0.4	3.624	6.679	5.568	1.450	0.543	0.295
	0.5	4.482	2.452	2.439	1.186	0.496	0.296

Source: own study.

Stream microparameters were measured at the point where the highest spray intensities were recorded. Studies [31,37] suggested that spiral nozzles forming a cone-shaped spray pattern have the largest average diameter values in the zone where the largest amount of water is applied. Differences in mean diameter values directly under the nozzle and in the main spray ring can exceed 150 µm [37]. For this reason, the microstructure of the jet produced by the NF 15 nozzle was tested at measuring point 1, while the TF6 NN and TF6 FCN nozzles were tested at measuring point 3 (Figure 3).

Results of tests of the average droplet diameters of the tested nozzles are presented in Table 2. The droplet size distribution related to surface diameters (spray spectrum) are shown in Figures 6–8.

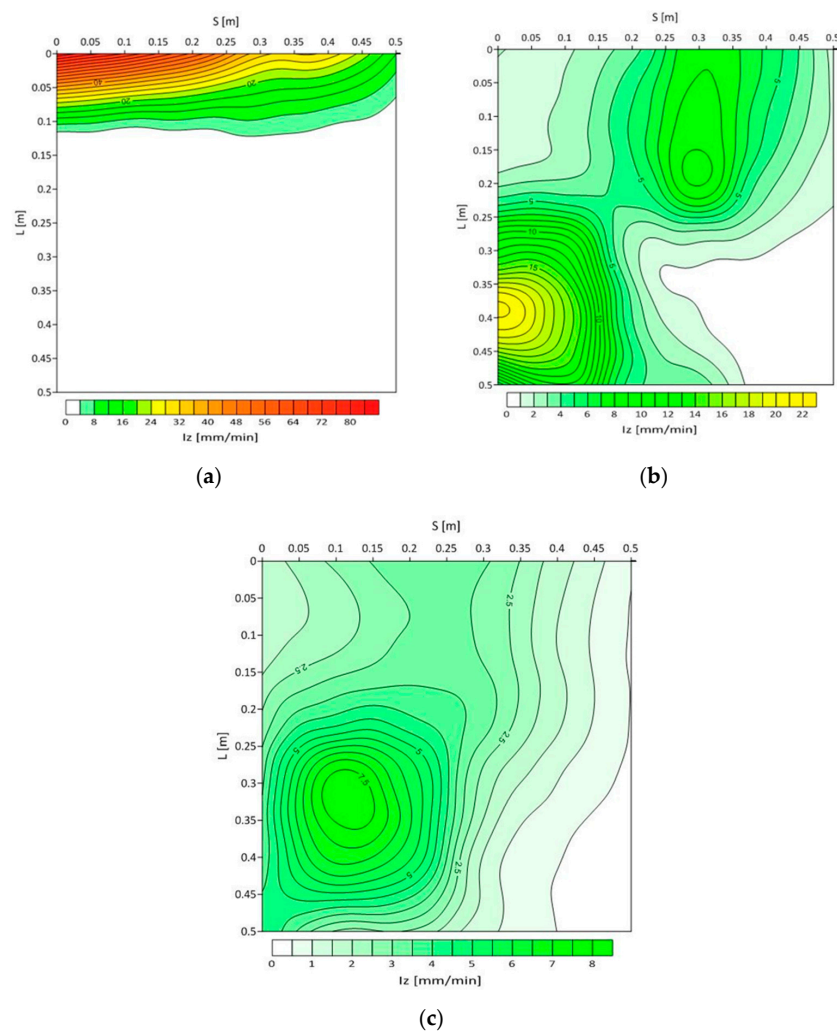


Figure 5. Spray intensity distributions of the tested nozzles: (a) TF6 NN, (b) NF15, (c) TF 6 FCN. Source: own study.

Table 2. Values of mean diameters of droplets produced by tested nozzles.

Parameter	Unit	Symbol	Nozzle Type		
			NF 15	TF 6 FCN	TF 6 NN
Number of counted droplets	pc.	N	414,099	87,376	157,886
Measurement time	sec.	t	180	180	180
Average quantitative diameter	μm	D_n	428.4	326.7	297
Average surface diameter	μm	D_s	535.7	393.7	375.8
Average volumetric diameter	μm	D_v	637	447.7	450.1
Maximum surface diameter	μm	$D_{s0.90}$	1482.5	866.5	1125
Nozzle supply pressure (average)	MPa	p	0.3026	0.3010	0.3011
Standard deviation of pressure measurement	MPa	σ_p	0.0007	0.0004	0.0005
Nozzle output (average)	dm^3/h	Q	367.43	353.06	328.59
Standard deviation of output measurement	dm^3/h	σ_Q	0.011	0.569	0.773

Source: own study.

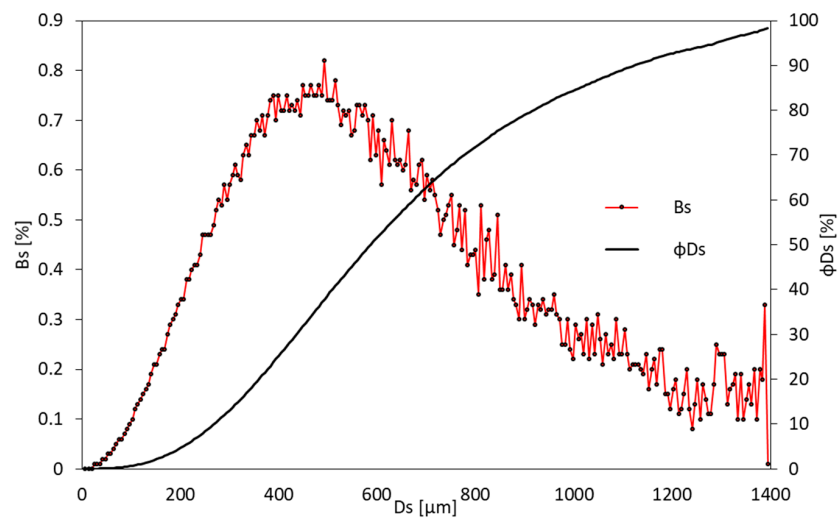


Figure 6. Spray spectrum for the nozzle TF6 NN. Source: own study.

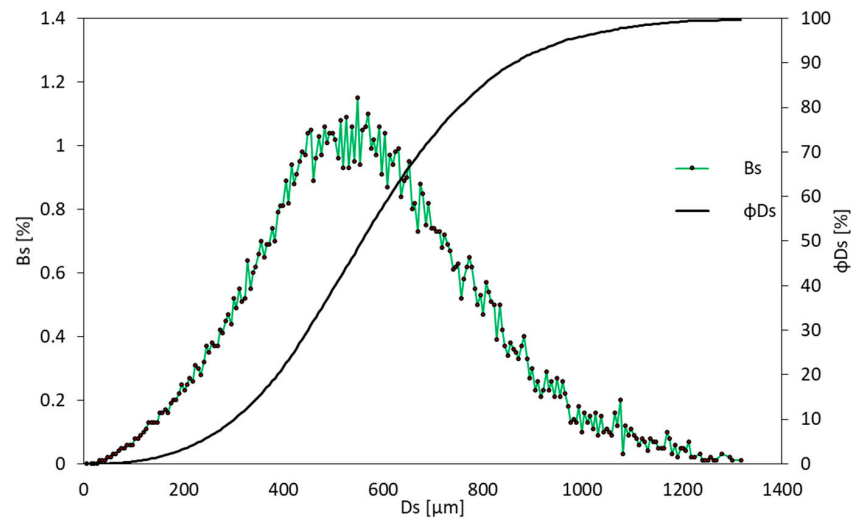


Figure 7. Spray spectrum for the nozzle TF6 FCN. Source: own study.

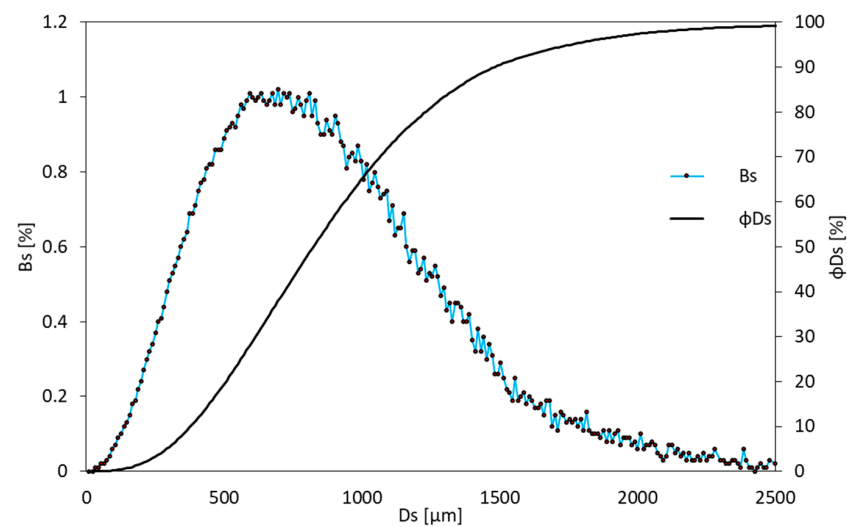


Figure 8. Spray spectrum for the nozzle TF6 NN. Source: own study.

The conducted microstructure studies suggest that the jet produced by a flat spray nozzle is characterised by the lowest dispersion. As compared to spiral nozzles, the value of average surface diameters is approximately 150 μm higher. In addition, the NF 15 nozzle exhibits a high inhomogeneity of droplet fragmentation. This is reflected in the range of the spray spectrum and the large $D_{S_{0.90}}$ value, which is close to 1.5 mm. The small dispersion of droplets and large variation in their diameters in the case of the NF 15 nozzle may be a result of the lack of turbulence in the jet produced by the nozzle, as well as from the large amount of water in the stream, as was confirmed by the spray intensity test.

Streams produced by spiral nozzles have similar average diameters. However, a greater spray uniformity was obtained for the TF 6 FCN nozzle, which was found to generate a stream with a small proportion of droplets with large diameters and a low value of $D_{S_{0.90}}$. The proportion of droplets with diameters of more than 1 mm is in this case less than 5% (in relation to surface diameters), while for the TF 6 NN nozzle, it is more than 15%. This implies that the change in the dispersion angle of spiral nozzles not only increases the uniformity of sprinkling, but also makes the distribution more uniform and improves the dispersion of the created stream.

The values of NH_3 concentration as a function of water application time for the nozzles used in the test, $C = f(t)$, are shown in Figure 9. They prove that the absorption process is the most dynamic when water is fed through the TF 6 FCN nozzle, and the slowest in the case of the NF 15 nozzle. The shape of the curves $C = f(t)$ corresponds to an exponential relation, which confirms the validity of the assumptions given in the literature [15]. After converting the concentration values into the logarithmic scale, straight lines $\ln C = f(t)$ reflecting the maximum kinetics of the absorption process could be established. The kinetic range of the straight line $\ln C = f(t)$ was determined in such a way that the determination coefficient was above 0.99. The ammonia absorption curves in the designated kinetic section are presented in Figure 10.

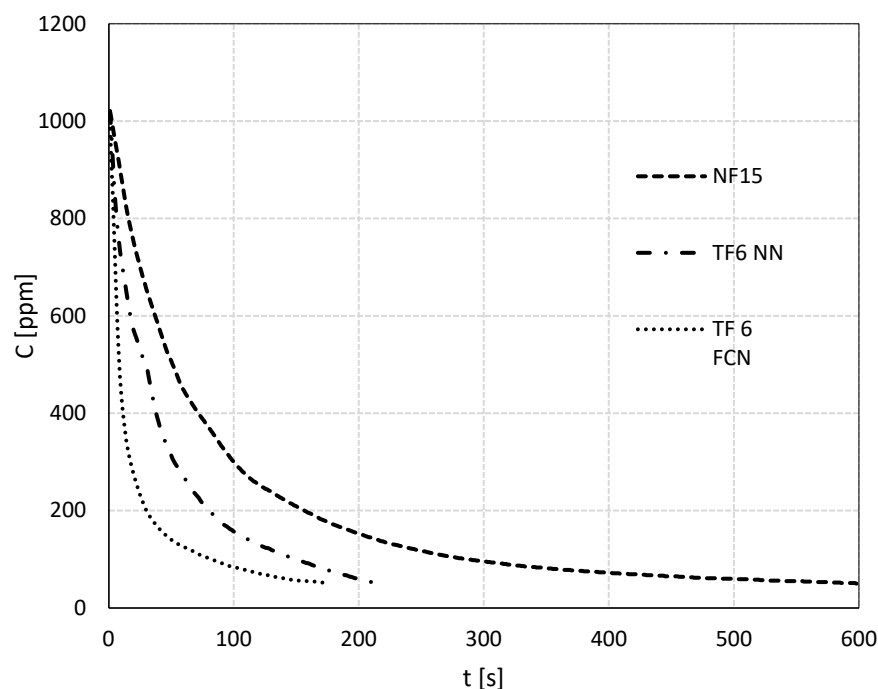


Figure 9. Change in ammonia concentration over time as water is fed through the test nozzles. Source: own study.

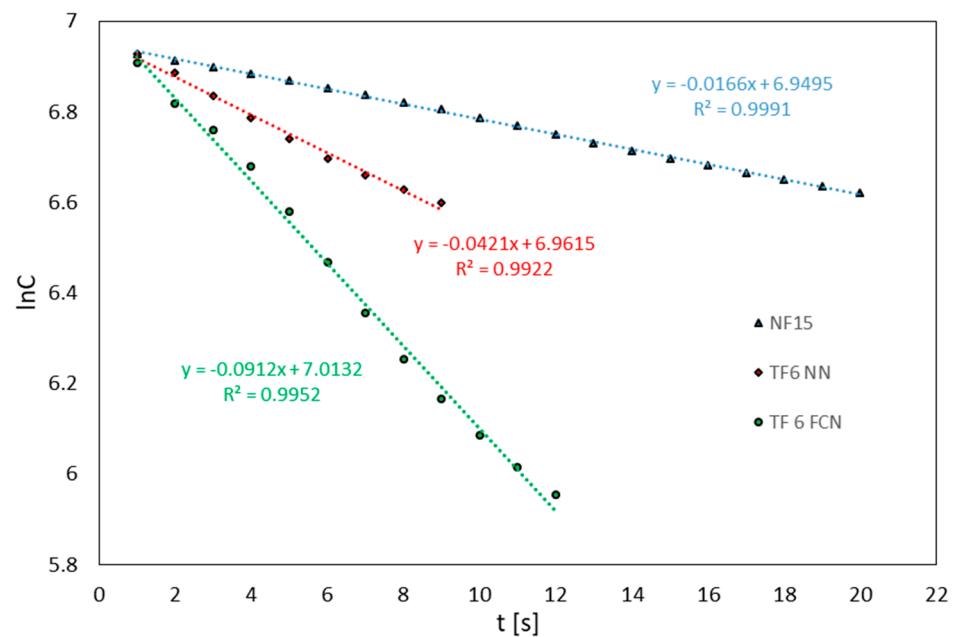


Figure 10. Ammonia absorption curves in the kinetic range. Source: own study.

The derived directional coefficients of straight lines $\ln C = f(t)$ reflect the apparent absorption rate constants k_p . On their basis, the concentration half-time was determined for each of the tested nozzles (Table 3).

Table 3. Results of the ammonia absorption parameters for the tested nozzles.

Parameter	Unit	Nozzle		
		NF15	TF6 NN	TF 6 FCN
$t_{1/2}$	s	41.81	16.47	7.60
k_p	s^{-1}	0.0166	0.0421	0.0912

Source: own study.

The obtained values of apparent constant for the absorption process rate and the concentration half-time in the kinetic range are similar to the data obtained by other investigators. In the case of studies [16] recorded were $k_p = 0.0521 \text{ s}^{-1}$ and $t_{1/2} = 13.29 \text{ s}$, while in studies [12] $k_p = 0.0361 \text{ s}^{-1}$ and $t_{1/2} = 20 \text{ s}$. The noted differences are due to the use of different types of spray nozzles and test conditions, including initial ammonia concentration and flow rate.

Testing the absorption of ammonia with different streams shows that the speed of the process characterized by the parameters k_p and $t_{1/2}$ depends on the structure of the water stream. In the results obtained with different water streams (Table 3), one should emphasise the large differences in the obtained values of the parameters that define the process rate. This indicates that micro- and macro-parameters of water streams significantly influence the efficiency of ammonia absorption.

It was found that, despite a slightly larger average surface diameter of the droplets of the jet produced with the TF 6 FCN nozzle ($393.7 \mu\text{m}$) than that of the TF 6 NN nozzle ($375.8 \mu\text{m}$), its efficiency in the case of ammonia absorption is significantly higher. The main reason for this is probably that in the jet produced by TF 6 FCN, there is a very small proportion of droplets with large diameters. Moreover, the improved efficiency of ammonia absorption by streams produced by the TF6 FCN nozzle is also influenced by the fact that this stream was characterised by the largest volume and the highest uniformity of spraying. The obtained results confirm that the evaluation of the absorption efficiency based only on the value of average droplet diameters is not always sufficient.

The unfavourable values for the parameters k_p and $t_{1/2}$ ascertained for the NF 15 nozzle arise from the fact that it generates a stream in a small volume, which is not conducive to jet dispersion. In addition, the flat shape of the jet does not positively influence the surface of interaction of the jet with the atomised gas. This is confirmed by the results of studies [44,45], in which it has been demonstrated that a stream with finer droplets acquires a larger total surface area, which has a direct effect on accelerating the penetration of ammonia into the droplets.

It should be noted that even the lowest k_p and $t_{1/2}$ values obtained for the stream coming from the NF 15 nozzle are significantly higher than the results obtained in tests carried out for other substances, such as acetone [15], methanol or 1-propanol [14] (amounting to $k_p = 0.0057 \text{ s}^{-1}$ and $t_{1/2} = 122$, $k_p = 0,00506 \text{ s}^{-1}$ and $t_{1/2} = 137 \text{ s}$, $k_p = 0,00132 \text{ s}^{-1}$ and $t_{1/2} = 523 \text{ s}$ respectively). This confirms that the absorption of ammonia by dispersed water jets is an effective method for eliminating this type of air pollution.

4. Conclusions

On the basis of the conducted research and interpretation of its results, confirmation has been found for many phenomena and laws connected with absorption of hazardous substances in water. Moreover, the adopted research assumptions consisting of elimination of several variables allowed the formulation of more precise conclusions and observations than those described so far in the literature. The trials were conducted at a constant initial ammonia concentration, nozzle supply pressure, flow rate, water temperature and ambient temperature. This allowed a more accurate assessment of how the parameters of micro- and macrostructure of the water stream affect the course of ammonia absorption. The following conclusions may be drawn:

- (1) Water streams with high inhomogeneity have a lower absorption efficiency. This is due to the fact that in areas with locally high spray intensities, streams with large mean droplet diameters and a wide spray spectrum are created.
- (2) For the absorption of a spatial ammonia cloud, nozzles forming jets with full spray cones should be used. In particular, these should be nozzles that form jets with a significant spray uniformity and a high dispersion.
- (3) For the elimination of risks associated with potential uncontrolled releases of ammonia, flat water jets can only be used as containment barriers intended to limit the spreading of pollutants. Such jets should be considered ineffective in case of absorption in the air.
- (4) An assessment of the influence of microparameters on absorption efficiency based only on mean droplet diameters may not be sufficient. The study shows that there may be cases in which streams with larger average droplet diameters will exhibit greater gaseous absorption capacity. This is related to the uniformity of the droplet dispersion in the stream.
- (5) Increasing the angle of dispersion in the cone jet improves the quality of water atomisation and increases the absorption of ammonia.
- (6) The use of inappropriate parameters of the water stream during ammonia absorption may lead to a few-fold slowing down of the process. This will definitely have a significant impact on the spread of the contamination and the area of the dangerous zone for people and the environment.

Author Contributions: W.W.: methodology and results development, measurements, gravimetric analysis, results processing. W.R.-K.: concept, results processing. M.M.-Ł.: statistical analysis, results processing. All authors have read and agreed to the published version of the manuscript.

Funding: The research was carried out as part of the DOB-BIO6/06/113/2014 project “Mobile turbine rescue and firefighting system” financed by The National Centre for Research and Development in Poland (NCBR). This research was partially funded from a subsidy of the Ministry of the Interior and Administration, Poland to The Main School of Fire Service in Warsaw, Poland.

Institutional Review Board Statement: Not applicable.

Informed Consent Statement: Not applicable.

Data Availability Statement: The code generated during the study and experimental data are available from the corresponding author by request.

Conflicts of Interest: Authors declare no conflicts of interest.

References

1. Mi, Y.; Ma, Y. Ultra-Highly Sensitive Ammonia Detection Based on Light-Induced Thermoelastic Spectroscopy. *Sensors* **2021**, *21*, 4548. [CrossRef] [PubMed]
2. Majder-Łopatka, M.; Węsierski, T. Liquidation of ammonia clouds using a mobile turbine rescue and firefighting system. *MATEC Web Conf.* **2018**, *46*, 00023. [CrossRef]
3. Fedoruk, M.J.; Bronstein, R.; Kerger, B.D. Ammonia exposure and hazard assessment for selected household cleaning product uses. *J. Expo. Anal. Sci. Environ. Epidemiol.* **2005**, *15*, 534–544. [CrossRef] [PubMed]
4. Ubowska, A. Environmental Hazard Related to a Rail Accident of a Tanker Transporting the Ammonia. *Sci. Pap. Main Sch. Fire Serv.* **2018**, *66*, 51–63. (In Polish). Available online: <https://zeszytynaukowe-sgsp.pl/resources/html/article/details?id=207827> (accessed on 1 May 2022).
5. Jiménez, I.; Vilà, A.M.; Calveras, A.C.; Morante, J.R. Gas sensing properties of catalytically modified WO_3 with copper and vanadium for NH_3 detection. *IEEE Sens. J.* **2002**, *5*, 385–391. [CrossRef]
6. Ubowska, A. Ammonia in cooling installations for the agri-food industry. *Work. Saf. Cent. Inst. Labor Prot.-Natl. Res. Inst.* **2016**, *1*, 14–17. (In Polish)
7. Główny Urząd Statystyczny. Rocznik Statystyczny Przemysłu (Central Statistical Office. Statistical Yearbook of Industry) 2018, 2019, 2020 and 2021. Available online: <https://stat.gov.pl/> (accessed on 1 May 2022).
8. International Fertiliser Association. Available online: <https://www.ifastat.org/supply/Nitrogen%20Products/Ammonia> (accessed on 1 May 2022).
9. Serafini, M.; Mariani, F.; Gualandi, I.; Decataldo, F.; Possanzini, L.; Fraboni, B.; Tonelli, D.; Scavetta, E. A wearable electrochemical gas sensor for ammonia detection. *Sensors* **2021**, *21*, 7905. [CrossRef]
10. Farren NJ; Davison J; Rose, R.A.; Wagner, R.L.; Carslaw, D.C. Underestimated Ammonia Emissions from Road Vehicles. *Environ. Sci. Technol.* **2020**, *54*, 15689–15697. [CrossRef]
11. Majder-Łopatka, M.; Węsierski, T.; Walczak, A. The use of the turbine rescue and firefighting system to limit the consequences of ammonia leakage from pressurised and non-pressurised storage tanks. *Logistyka* **2015**, *5*, 1121–1127. (In Polish)
12. Majder-Łopatka, M.; Węsierski, T.; Wąsik, W. Effect of Nozzle Structure on the Absorption Efficiency of the Ammonia Cloud Formed as a Result of Industrial Accidents. *Saf. Fire Technol.* **2016**, *42*, 127–134. (In Polish)
13. Węsierski, T. Effectiveness of water curtains during fighting against vapors of saturated linear low molecular mass alcohols during its uncontrolled release. *Chem. Ind.* **2015**, *5*, 728–730. (In Polish)
14. Węsierski, T.; Majder-Łopatka, M.; Wąsik, W. Control of ammonia space contaminations by using turbine fire-fighting vehicles. *Chem. Ind.* **2017**, *96*, 1080–1084. (In Polish)
15. Węsierski, T. Study of water curtain effectiveness to fight against vapors of acetone during uncontrolled release. *Chem. Ind.* **2017**, *96*, 1539–1542. (In Polish)
16. Węsierski, T.; Majder-Łopatka, M. Comparison of water curtain effectiveness in the elimination of airborne vapours of ammonia, acetone, and low-molecular aliphatic alcohols. *Appl. Sci.* **2018**, *8*, 1971. [CrossRef]
17. Węsierski, T.; Majder-Łopatka, M.; Matuszkiewicz, R.; Porowski, R. Study on the effectiveness of water curtains to control of ammonia vapors during its uncontrolled release. *Chem. Ind.* **2012**, *91*, 1424–1426. (In Polish)
18. Hua, M.; Qi, M.; Yue, T.-T.; Pi, X.-Y.; Pan, X.-H.; Jiang, J.-C. Experimental Research on Water Curtain Scavenging Ammonia Dispersion in Confined Space. *Procedia Eng.* **2018**, *211*, 256–261. [CrossRef]
19. Cheng, C.; Tan, W.; Du, H.; Liu, L. A modified steady-state model for evaluation of ammonia concentrations behind a water curtain. *J. Loss Prev. Process Ind.* **2015**, *36*, 120–124. [CrossRef]
20. Isnard, O.; Soulhac, L.; Dusserre, G. Numerical simulation of ammonia dispersion around a water curtain. *J. Loss Prev. Ind.* **1999**, *12*, 471–477. [CrossRef]

21. Dandrieux, A.; Dusserre, G.; Ollivier, J.; Fournet, H. Effectiveness of water curtains to protect firemen in case of an accidental release of ammonia: Comparison of the effectiveness for two different release rates of ammonia. *J. Loss Prev. Process Ind.* **2001**, *14*, 349–355. [[CrossRef](#)]
22. Shen, X.; Zhang, J.; Hua, M.; Pan, X. Experimental research on decontamination effect of water curtain containing compound organic acids on the leakage of ammonia. *Process Saf. Environ. Prot.* **2017**, *105*, 250–261. [[CrossRef](#)]
23. Rana, M.A.; SamMannan, M. Forced dispersion of LNG vapor with water curtain. *J. Loss Prev. Process Ind.* **2010**, *23*, 768–772. [[CrossRef](#)]
24. Warych, J. *Oczyszczanie Gazów. Procesy i Aparatura*, 1st ed.; WNT: Warsaw, Poland, 1998. (In Polish)
25. Warych, J. *Oczyszczanie Przemysłowych Gazów Odlotowych*; PWN: Warsaw, Poland, 1994. (In Polish)
26. Warych, J. *Odpylanie Gazów Metodami Mokrymi*; WNT: Warsaw, Poland, 1979. (In Polish)
27. Zbrożek, P.; Prasula, J. Influence of water mist drop size on efficiency of fire suppression and cooling. *Saf. Fire Technol.* **2009**, *3*, 113–148. (In Polish)
28. Ochowiak, M.; Krupinska, A.; Włodarczak, S.; Matuszak, M.; Woziwodzki, S.; Szulc, T. Analysis of the possibility of disinfecting surfaces using portable foggers in the era of the SARS-CoV-2 epidemic. *Energies* **2021**, *14*, 2019. [[CrossRef](#)]
29. Catalog Card Nozzles TF. Available online: <https://www.bete-dysze.pl/files/bete-duesen-de/pdf/vollkegel/tf.pdf> (accessed on 1 May 2022).
30. Catalog Card Nozzles NF. Available online: <https://www.bete-dysze.pl/files/bete-duesen-de/pdf/flachstrahl/nf.pdf> (accessed on 1 May 2022).
31. Majder-Łopatka, M.; Węsierski, T.; Wasik, W.; Binio, L. Effects of the supply pressure in a spiral vortex nozzle on a dispersion angle and the sprinkling density of water jet. *Sci. Pap. Main Sch. Fire Serv.* **2017**, *61*, 137–151. (In Polish)
32. Orzechowski, Z.; Prywer, J. *Wytwarzanie i Zastosowanie Rozpylonej Cieczy* Wydawnictwo Naukowe; PWN SA: Warszawa, Poland, 2018. (In Polish)
33. *Instrukcja Obsługi Analiza Widma Kropel IPS*; Zakład Elektronicznej Aparatury Pomiarowej Firma KAMIKA Instruments Sp. z o.o. Sp.k.: Warsaw, Poland, 2009.
34. Ochowiak, M.; Włodarczak, S.; Krupinska, A.; Matuszak, M.; Fedak, W.; Ligus, G.; Kołodziej, S.; Wasilewska, B. Spray curtains as devices for surface spraying during the SARS-CoV-2 pandemic. *Environ. Res.* **2022**, *206*, 112562. [[CrossRef](#)] [[PubMed](#)]
35. Kubica, P.; Gałaj, J. Comparative analysis of the effectiveness of water spraying through selected fog nozzles. *Sci. Pap. Main Sch. Fire Serv.* **2004**, *31*, 37–48. (In Polish). Available online: https://www.sgsp.edu.pl/?page_id=1847 (accessed on 1 May 2022).
36. Gałaj, J.; Kieliszek, S.; Drzymała, T. Investigation of the influence of the swirling of the central jet of a selected nozzle on the parameters of an atomized stream. *Sci. Pap. Main Sch. Fire Serv.* **2007**, *35*, 5–17. (In Polish). Available online: <https://www.infona.pl/resource/bwmeta1.element.baztech-c693334e-3318-47f2-aa0c-ba48c2b32bbe/content/partContents/6831e257-c981-3ede-a380-0ac2f7770f5e> (accessed on 1 May 2022).
37. Wasik, W.; Rogula-Kozłowska, W.; Majder-Łopatka, M. Evaluation of the microstructure of water jet produced by a full cone spiral nozzle. *Sci. Pap. Main Sch. Fire Serv.* **2021**, *79*, 105–122. (In Polish)
38. Orzechowski, Z.; Prywer, J. *Wytwarzanie i Zastosowanie Rozpylonej Cieczy*, 1st ed.; WNT: Warsaw, Poland, 2008.
39. *Instrukcja Obsługi. Miernik Wielogazowy MX6 iBrid*, 4th ed.; Cat. No. 17130279-A; Industrial Scientific: Pittsburgh, PA, USA, 2014.
40. Majder-Łopatka, M.; Węsierski, T.; Dmochowska, A.; Ilnicki, M. Photoionization Detectors (PID) in the Fire Safety. *Sci. Pap. Main Sch. Fire Serv.* **2014**, *49*, 59–66.
41. Majder-Łopatka, M.; Węsierski, T.; Dmochowska, A.; Salamonowicz, Z.; Polańczyk, A. The Influence of Hydrogen on the Indications of the Electrochemical Carbon Monoxide Sensors. *Sustainability* **2019**, *12*, 14. [[CrossRef](#)]
42. Majder-Łopatka, M. Effects of interfering gases in electrochemical sensors NH₃ and NO₂. *MATEC Web Conf.* **2018**, *247*, 00023. [[CrossRef](#)]
43. Buchlin, J.-M. Thermal shielding by water spray curtain. *J. Loss Prev. Process Ind.* **2005**, *18*, 423–432. [[CrossRef](#)]
44. Fedak, W.; Ulbrich, R.; Ligus, G.; Wasilewski, M.; Kołodziej, S.; Wasilewska, B.; Ochowiak, M.; Włodarczak, S.; Krupinska, A.; Pawlenko, I. Influence of Spray Nozzle Operating Parameters on the Fogging Process Implemented to Prevent the Spread of SARS-CoV-2 Virus. *Energies* **2021**, *14*, 4280. [[CrossRef](#)]
45. Ochowiak, M.; Krupinska, A.; Włodarczak, S.; Matuszak, M.; Markowska MJanczarek, M.; Szulc, T. The two-phase conical swirl atomizers: Spray characteristics. *Energies* **2020**, *13*, 3416. [[CrossRef](#)]